
pinta: The uGMRT Data Processing Pipeline for the Indian Pulsar Timing Array

Abhimanyu Susobhanan^{1*}, Yogesh Maan², Bhal Chandra Joshi³, T. Prabu⁴, Shantanu Desai⁵, Yashwant Gupta³, A. Gopakumar¹, Neelam Dhanda Batra⁶, Arpita Choudhary⁷, Mayuresh P. Surnis⁸, Lankeswar Dey¹, Jaikhomba Singha⁹, K. Nobleson¹⁰, Manjari Bagchi^{7,11}, Avishek Basu³, Suryarao Bethapudi¹², Kishalay De¹³, Raghav Girgaonkar⁵, M. A. Krishnakumar¹⁴, P. K. Manoharan¹⁵, Arun Kumar Naidu¹⁶, Dhruv Pathak^{7,12}, Sai Chaitanya Susarla¹⁷

¹Department of Astronomy and Astrophysics, Tata Institute of Fundamental Research, Dr. Homi Bhabha Road, Mumbai 400005, Maharashtra, India

²Anton Pannekoek Institute, University of Amsterdam, Postbus 94249, 1090 GE Amsterdam, The Netherlands

³National Centre for Radio Astrophysics, Tata Institute of Fundamental Research, Ganeshkhind, Pune 411007, Maharashtra, India

⁴Raman Research Institute, Bengaluru 560080, Karnataka, India

⁵Department of Physics, Indian Institute of Technology Hyderabad, Kandi, Telangana 502285, India

⁶Department of Physics, Indian Institute of Technology Delhi, New Delhi-110016, India

⁷The Institute of Mathematical Sciences, C. I. T. Campus, Tharamani, Chennai 600113, Tamil Nadu, India

⁸Jodrell Bank Centre for Astrophysics, University of Manchester, Oxford Road, Manchester, M13 9PL, UK

⁹Department of Physics, Indian Institute of Technology Roorkee, Roorkee 247667, Uttarakhand, India

¹⁰Department of Physics, BITS Pilani Hyderabad Campus, Hyderabad 500078, Telangana, India

¹¹Homi Bhabha National Institute, Training School Complex, Anushakti Nagar, Mumbai 400094, Maharashtra, India

¹²Department of Physics and Astronomy, University of Texas, Rio Grande Valley, Brownsville, TX 78520, USA

¹³Cahill Center for Astrophysics, California Institute of Technology, 1200 E. California Blvd. Pasadena, CA 91125, USA

¹⁴Fakultät für Physik, Universität Bielefeld, Postfach 100131, D-33501 Bielefeld, Germany

¹⁵Arecibo Observatory, University of Central Florida, Arecibo, FL 32816, USA

¹⁶McGill Space Institute, McGill University, 3550 University Street, Montréal, QC H3A 2A7, Canada

¹⁷Indian Institute of Science Education and Research Thiruvananthapuram, Maruthamala, Kerala 695551, India

Abstract

We introduce *pinta*, a pipeline for reducing the uGMRT raw pulsar timing data developed for the Indian Pulsar Timing Array experiment. We provide a detailed description of the workflow and usage of *pinta*, as well as its computational performance and RFI mitigation characteristics. Furthermore, the results of a calibration experiment carried out to determine the relative time offsets between different back-end modes and the correct interpretation of the observatory frequency settings at the uGMRT, which are crucial for performing precision pulsar timing, are also discussed.

Keywords: Astronomy data analysis – pulsars

1 INTRODUCTION

Ubiquitous galaxy mergers are expected to force their resident supermassive black holes to merge (Pearson et al., 2019; Berczik et al., 2006). During such merger and the preceding inspiral phases, the black hole pairs are expected to emit gravitational waves (GWs) in the nanohertz frequency range (Burke-Spolaor et al., 2019; Susobhanan et al., 2020). Pulsar Timing Arrays (PTAs; Hobbs & Dai, 2017) aim to detect such GWs by accurately timing the arrival of pulses from an ensemble of millisecond pulsars (MSPs) as these are very precise celestial clocks (Hobbs et al., 2020). The most promising

PTA sources include isolated supermassive black hole binaries (SMBHBs) emitting continuous GWs and an astrophysical stochastic GW background formed from an ensemble of many unresolved SMBHBs (Burke-Spolaor et al., 2019). Their eventual detections will augment an additional window to the GW astronomy landscape inaugurated by the LIGO-Virgo collaboration (Abbott et al., 2019). At present, there exist three matured PTA experiments, namely the Parkes Pulsar Timing Array (PPTA; Hobbs, 2013; Kerr et al., 2020), the European Pulsar Timing Array (EPTA; Kramer & Champion, 2013; Desvignes et al., 2016), and the North American Nanohertz Observatory for Gravitational Waves

*s.abhimanyu@tifrr.res.in

(NANOGrav: McLaughlin, 2013; Alam et al., 2020a,b). Additionally, PTA efforts are gaining momentum in India, China and South Africa (Joshi et al., 2018; Lee, 2016; Bailes et al., 2018), and these collaborations are referred to as the emerging PTAs. The International Pulsar Timing Array (IPTA) consortium combines data and resources from various PTA efforts to enable faster detection of nanohertz GWs (Hobbs et al., 2010; Perera et al., 2019).

The Indian Pulsar Timing Array (InPTA) experiment, operational since 2015 (Joshi et al., 2018), aims to use the unique strengths of the Giant Metrewave Radio Telescope (GMRT: Swarup et al., 1991)—especially after its recent upgrade (uGMRT: Gupta et al., 2017)—along with the Ooty Radio Telescope (ORT: Swarup et al., 1971; Naidu et al., 2015) to complement the other PTA experiments. The uGMRT, with its ability to observe below 1 GHz, is an ideal instrument to characterize inter-stellar medium effects such as dispersion measure (DM) variations of PTA pulsars, which is necessary to achieve the nanosecond timing precision required for the first detection of nanohertz GWs (Joshi et al., 2018).

The first step in using uGMRT and ORT data for InPTA science goals is to reduce it to an *archive* format (Hotan et al., 2004) – a pulsar data format widely used among other PTAs. Then, these data can be further processed using well-known software to derive various astrophysically relevant quantities including the pulse time of arrival (TOA) and the DM (van Straten et al., 2012). This calls for homogeneity in data reduction practices to avoid non-uniformity in the data products used for PTA analysis, which can introduce systematic errors. In this paper, we describe a uGMRT pulsar data analysis pipeline named “Pipeline for the Indian Pulsar Timing Array” (`pinta`¹), developed for the InPTA experiment to address these concerns as well as to improve the efficiency, reliability, and user friendliness of the data reduction process and to ensure faster turnaround time from observations to PTA analysis.

We intend to commission `pinta` as an observatory pipeline at GMRT to be used by the wider pulsar community. This can help avoid transfer of large data files by enabling data reduction at the observatory itself. For the pipeline to be useful to a wider community, we also discuss how to interpret the uGMRT observation frequency settings, along with our astronomical experiments performed to deduce and validate the presented interpretation. Using the same experiment, we also deduced the instrumental delays between various back-end modes used at uGMRT. These delays form a crucial piece of information, not only for combining data from multiple bands in the InPTA analysis, but also for other simultaneous multi-frequency observations which use different back-end modes.

The outline of this paper is as follows. A detailed description of the uGMRT raw data as well as the workflow and usage of `pinta` is provided in Section 2. Details of the uGMRT observation frequency settings and the astronomical experiments which were used to deduce and validate these settings are presented in Section 3. The performance and RFI mitigation characteristics of `pinta` are reported in Section 4. A summary of various aspects of the `pinta` pipeline discussed in this paper is given in Section 5 and our future plans for the development of InPTA-relevant codes including `pinta` are summarized in Section 6.

2 DESCRIPTION OF THE PIPELINE

`pinta` accepts uGMRT raw pulsar timing data as input, performs RFI mitigation and folding, and provides the partially folded pulse profile in the `Timer` archive format (van Straten & Bailes, 2011) as its output. In what follows, we give a detailed description of the uGMRT raw data and the workflow of the `pinta` pipeline.

The GMRT antennae are divided in groups to form multiple subarrays, and each subarray is phased to form voltage beams for two polarizations. These voltage beams are then digitized and Fourier transformed to form power spectra across a certain number of frequency channels (Reddy et al., 2017). For the phased array (PA) mode that we use in our InPTA timing observations, the spectra from the two polarizations are combined to form the total intensity (I), and is integrated maintaining the required spectral and time resolution for the observation specified in terms of the number of channels N_{chan} and the sampling time T_{smp} . Note that the polarization voltages can also be combined to compute the Stokes parameters (I, Q, U, V ; Hamaker et al., 1996). While recording of the full Stokes data is possible at uGMRT, the implementation of its reduction in the pipeline described here is currently being developed and tested. In addition, a real-time coherent dedispersion observing mode can be employed to process the voltages to form and record the coherently dedispersed phased array (CDPA) raw data stream (De & Gupta, 2016). Lastly, an incoherent array (IA) data stream can be formed by incoherently adding the spectral powers from different antennae.

The PA and the CDPA total intensity modes are used for InPTA observations. The CDPA mode is primarily used at the lower frequency bands, where the effect of interstellar dispersion is prominent. The raw data stream from either of these modes, namely a data cube of spectral intensities at N_{chan} frequency channels for each time sample, are stored as 16-bit integers in a binary raw data file, and the timestamp (in Indian Standard Time) at the start of observation is saved as a separate ASCII file. An example timestamp file is shown below.

¹Available at <https://github.com/abhiskck1/pinta>.

```
#Start time and date
IST Time: 19:59:57.633098240
Date: 25:08:2018
#Start ACQ SEQ NO = 17
```

Note that the raw data files do not store any meta-data required for downstream processing and it must be provided to the pipeline through a separate file.

Reduction of PTA data involves processing large number of such huge datasets (obtained towards different MSPs and at different epochs) through complex processing steps. In order to ensure that processing can be efficient for such batch processing jobs and to avoid premature failures, a set of sanity checks are done on all the relevant files and folders, and the processing is initiated only if all the checks pass. If one of the checks fail, an informative error message is shown to enable easier troubleshooting.

The data processing workflow of *pinta* is illustrated in Figure 1. *pinta* uses two separate packages for RFI mitigation, namely *gptool*² (Chowdhury & Gupta, 2020) and *rfiClean*³ (Maan et al., 2020). Brief descriptions of these packages are given below.

gptool is both an RFI mitigation and data reduction tool for the beamformer data from the GMRT. It mitigates both narrow-band spectral line RFI and broadband bursty time-domain RFI. For the former, it offers a choice of two options for flagging RFI-affected frequency channels: (a) it derives a median band-shape and flags channels for which the median absolute deviation (MAD) from the median exceeds a defined threshold; or (b) it checks for drop in mean-to-rms ratio for each channel below a specified threshold to identify channels corrupted by RFI. For identifying broadband RFI, *gptool* once again offers two options: (a) a standard MAD-based scheme of the individual time samples collapsed across the full bandwidth, or (b) a novel scheme for estimating the underlying statistics using the modal point and full width at half maximum calculations, which has been found to give much better results. For handling the flagged frequency channels and time samples, *gptool* again offers two options to the user: either replace by zero or replace by the local median. Both the filtered and unfiltered data are then dedispersed and folded to the ephemeris of the observed pulsar. When *gptool* is run in the interactive mode, the time-series, folded profile and the band-shape are displayed as the tool processes the raw data. *pinta* uses the non-interactive mode of *gptool*, where the filtered data in the same format as the input data is written to an output file along with estimated statistics in auxiliary files. *gptool* provides an option for the removal of a baseline computed by dedispersing the data to zero DM, useful for broadband RFI

mitigation, and an option for flattening the variations of the band-shape across the observing bandwidth by renormalizing the output of each frequency channel to the same mean value. The parameters for RFI removal and the selected modes are specified with a configuration file, named *gptool.in*. The tool has been extensively used for RFI mitigation in the uGMRT data for many pulsar projects since the first wide-band observations with the uGMRT.

rfiClean is useful in situations where the data is contaminated by periodic RFI, which could limit the efficacy of conventional RFI mitigation techniques. There are many terrestrial sources of periodic interference, the most infamous being the household 50/60 Hz power-lines. *rfiClean* identifies and mitigates periodic interference in the time series of individual frequency channels using Fourier domain analysis. After the excision of periodic interference, *rfiClean* uses the more conventional threshold-based techniques to identify the time samples as well as frequency channels respectively contaminated by broadband bursts and narrow-band RFI. The identified time samples and frequency channels are replaced by mean values, computed robustly in the local regions around the affected samples. *rfiClean* has been extensively and successfully tested against any artefacts which might get incorporated in the data during the periodic RFI excision, and might be relevant to the PTA analysis. The details of these tests can be found in Maan et al. (2020). Before inclusion in *pinta*, *rfiClean* was also independently tested as a stand-alone program using InPTA data, and was found to significantly enhance the quality of the reduced data and the timing analysis. *rfiClean* has also been used in several other completed and ongoing projects (e.g., Maan et al., 2019; Oostrum et al., 2020). For some pulsars with their spin frequency or any of its harmonics unfavourably close to 50/60 Hz, detection of the pulsar signal at several epochs was possible only after *rfiClean*'s mitigation of the periodic and other RFI.

While both the RFI mitigation packages have been well tested, the possibility of discovering a new artefact in the future cannot be ruled out. Hence, to avoid the need of re-analysing all the data in such an unlikely future situation, we have designed *pinta* such that it allows the user to process the data in two separate branches, one for each RFI mitigation package, and produces two separate outputs. Availability of data reduced by two independent parts of the pipeline facilitate detailed comparisons and the choice of optimal RFI mitigation method for each observation.

gptool accepts uGMRT raw data as input and writes the output in a similar format. The conversion to the filterbank format is carried out by a version of the *filterbank* command provided by the *sigproc* package (Lorimer, 2011), customized for uGMRT. On the other hand, *rfiClean* accepts input either in uGMRT

²Stands for GMRT Pulsar Tool

³Available at <https://github.com/ymaan4/rfiClean>

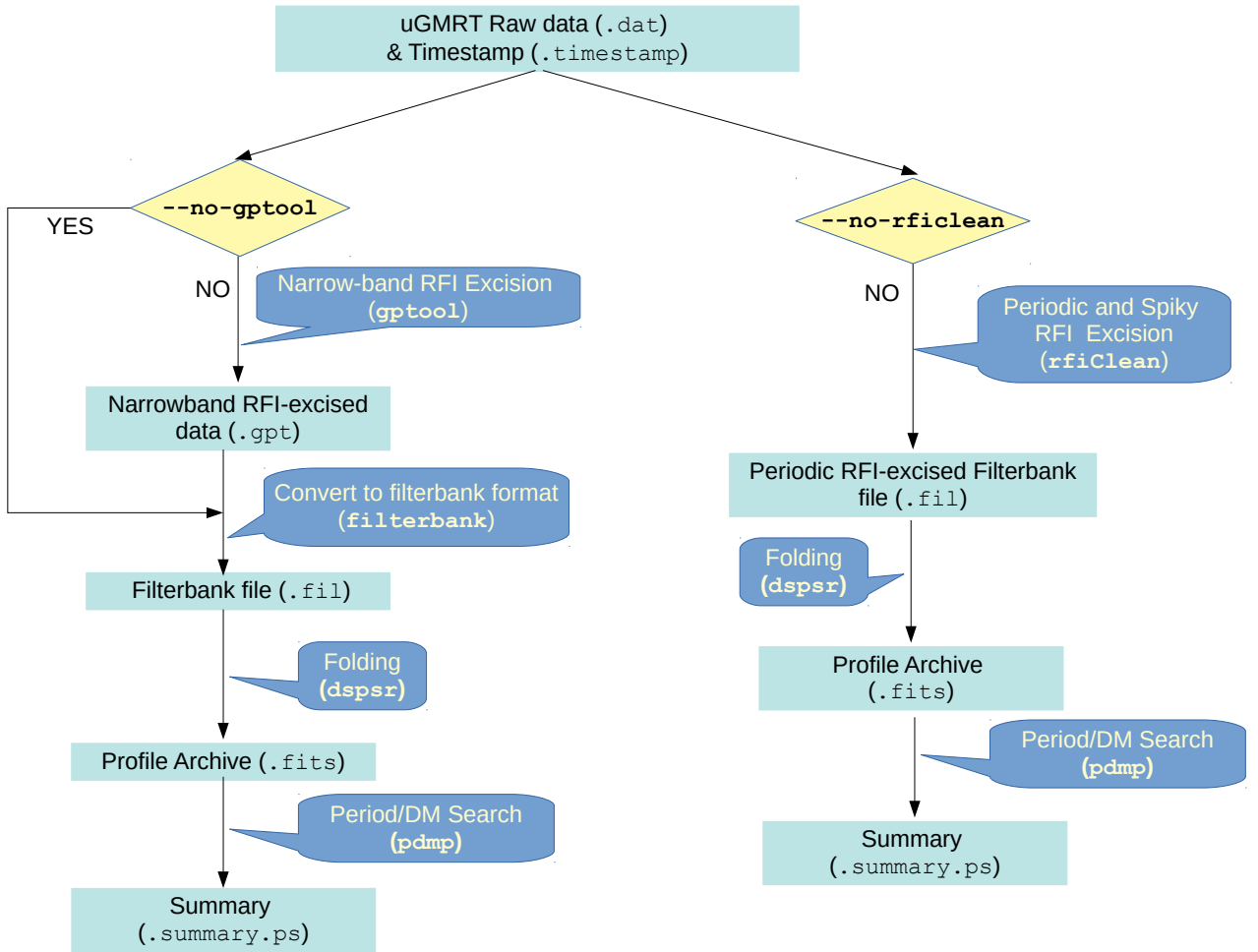


Figure 1. The workflow of pinta.

raw data format or in the `sigproc-filterbank` format, and outputs a `sigproc-filterbank` file.

The RFI-mitigated filterbank files are then folded using `dspsr` (van Straten & Bailes, 2011) and saved in the `Timer` format (the data can also be saved in `PSRFITS` format), significantly reducing the data volume. Finally, a period and DM search is performed on the resulting profile archive using the `pdmp` command provided by `psrchive`, producing a summary document in the `postscript` format. This file is used as a visual check to ensure that the pulsar has been detected and that the analysis has finished successfully.

2.1 Usage

The `pinta` pipeline can be invoked from the command line with the following syntax.

```
$ pinta [--help] [--test] [--no-gptool]
  [--no-rficlean] [--nodel] [--retain-aux]
  [--log-to-file] [--gptdir <...>]
  [--pardir <...>] [--rficconf <...>]
```

<input_dir> <working_dir>

`pinta` requires specifying two mandatory parameters and a few other optional parameters as inputs as listed below.

1. **Input directory** (`input_dir`) — The directory where the raw data files and the corresponding timestamp files are stored.
2. **Working directory** (`working_dir`) — The output files, as well as all the intermediate products, will be written to this directory. This directory must contain a file named `pipeline.in` as specified in subsection 2.3, and the user must have ‘read’ and ‘write’ permissions for this directory. The working directory can be the same as the input directory.
3. **gptool configuration directory** (`gpt_dir`) — This directory should contain the configuration files required to run `gptool`, named `gptool.in.xxx` where ‘xxx’ represents the local oscillator frequency of the uGMRT band. A detailed description of these files can be found in Chowdhury & Gupta (2020).

Argument	Description	Mandatory/ Optional
<i>Positional Arguments</i>		
<input_dir>	The input directory	Mandatory
<working_dir>	The working directory.	Mandatory
<i>Options</i>		
--help	Output a help message	Optional
--test	Do not execute data processing commands. All checks are performed on the input files and the commands are printed on the screen. This option is present for troubleshooting.	Optional
--no-gptool	Do not run <code>gptool</code> . Produces an output file without RFI mitigation.	Optional
--no-rficlean	Do not run <code>rfiClean</code> .	Optional
--nodel	The pipeline deletes all intermediate output files by default to conserve disk space. This option preserves the intermediate outputs.	Optional
--retain-aux	Components of the pipeline produce various side products in addition to the primary data products, which are removed by <code>pinta</code> by default. This option preserves these files by moving them to a folder named <code>aux</code> inside the <code>working_dir</code> .	Optional
--log-to-file	This option redirects the standard output generated from <code>pinta</code> to a log file in the <code>current_dir</code> .	Optional
--gptdir <...>	Specifies the directory where the <code>gptool</code> configuration files are stored. By default, this is specified in the configuration file (See subsection 2.2).	Optional
--pardir <...>	Specifies the directory where the pulsar ephemeris files are stored. By default, this is specified in the configuration file (See subsection 2.2).	Optional
--rficconf <...>	Specifies the <code>rfiClean</code> configuration file. By default, this is specified in the configuration file (See subsection 2.2).	Optional

Table 1 Command line options available in `pinta`.

- Pulsar ephemeris directory** (`par_dir`) — This directory should contain the pulsar ephemeris (`.par`) files in the `tempo2` format, required for folding the data. Each ephemeris file should be named `JNAME.par` where “JNAME” is the name of the pulsar in the J2000 epoch.
- rfiClean configuration file** (`rficconf_file`) — This file contains the settings and flags required to run `rfiClean` for `pinta`.

In addition, we shall refer to the directory from which `pinta` is invoked and directory where the `pinta` script is stored as the *current directory* (`current_dir`) and *script directory* (`script_dir`) respectively.

Note that both `working_dir` and the `current_dir` require write access. The `input_dir` and `working_dir` are mandatory positional arguments to be passed to `pinta`, while `gpt_dir`, `par_dir` and `rficconf_file` are by default read from a configuration file, detailed in the next subsection. `gpt_dir`, `par_dir` and `rficconf_file` can be explicitly specified in the command line through the `--gptdir`, `--pardir` and `--rficconf` options respectively. The various options and command line arguments are summarized in Table 1.

2.2 The Configuration File

The `pinta` configuration file stores the default settings required to run the pipeline, such as the `gpt_dir`, `par_dir` and `rficconf_file` in YAML format⁴. This file should be named `pinta.yaml` and stored in the `script_dir`.

A sample configuration file is shown below.

```
pinta:
  pardir: /path/to/pulsar/ephemeris/dir/
  gptdir: /path/to/gptool/config/dir/
  rficconf: /path/to/rfiClean/config/file/
```

2.3 The pipeline.in File

Since the input data files do not contain any metadata required for downstream processing, such as the number of channels and the bandwidth, it must be provided separately. `pinta` accepts this information through a space-separated ASCII file named `pipeline.in` stored in the `working_dir`. Each row in `pipeline.in` corresponds to one raw data file and the various columns are described in Table 2. Rows starting with “#” are treated

⁴<https://yaml.org/>

Column	Parameter	Description	Data Type	Unit
1	JName	The name of the pulsar in J2000 epoch.	String	
2	RawDataFile	Raw data file name. Only the file name is required and not the full path.	String	
3	TimestampFile	Timestamp file name. Only the file name is required and not the full path.	String	
4	Frequency (F_{LO})	Local oscillator frequency of the observing band.	Float	MHz
5	NBins (N_{bin})	Number of phase bins for the folded profile.	Integer	
6	NChans (N_{chan})	Number of frequency channels.	Integer	
7	BandWidth (ΔF)	Bandwidth of the observing band.	Float	MHz
8	TSample (T_{smp})	The sampling time used for observation.	Float	s
9	SideBand	The side-band. This should be either LSB (lower side-band) or USB (upper side-band).	String	
10	NPol (N_{pol})	Number of polarizations (1:=(I), 4:=(I,Q,U,V))	Integer	
11	TSubInt (T_{subint})	The duration of individual sub-integrations within which the data will be folded over the pulsar period.	Float	s
12	Cohded	Whether the data has been coherently dedispersed (De & Gupta, 2016). 1 represents Yes and 0 represents No.	Boolean	

Table 2 Description of various volumns in the `pipeline.in` file.

as comments and ignored. `pinta` processes rows in the `pipeline.in` files serially until all rows are processed successfully or a validation criterion is not met.

An example `pipeline.in` file is shown in Figure 2.

2.4 Storage Requirements

The uGMRT raw data file generated by an hour-long observation typically runs into few tens of Gigabytes. A uGMRT raw data file contains, for each time sample, N_{pol} polarization intensities/correlations in N_{chan} frequency channels represented as 16-bit integers. In general, the file size of the raw data file for an observation duration T_{obs} and sampling time T_{smp} is given by

$$S_{raw} = N_{pol}N_{chan} \frac{T_{obs}}{T_{smp}} \times 2 \text{ bytes}. \quad (1)$$

The intermediate products generated by the pipeline, namely, `.gpt` and `.fil` files, will have roughly the same size as the input file along with a small header which stores observation metadata. The output archives are typically smaller, of the order of hundreds of Megabytes in size, since we fold the raw data over longer sub-integrations. The size of the output archive, excluding the header, is approximately given by

$$S_{arch} \sim \frac{T_{smp}}{S_{subint}} N_{bin} S_{raw}, \quad (2)$$

where S_{subint} is the duration of a sub-integration and N_{bin} is the number of phase bins in the profile. In general, the maximum amount of disk space required by `pinta` is less than four times the total size of the raw data files, while preserving all intermediate files (i.e.,

using the `--node1` option). If the `--node1` option is not used, the maximum amount of disk space required is approximately the size of the largest raw data file.

3 INTERPRETATION OF OBSERVATORY FREQUENCY SETTINGS

The GMRT Wide-band Back-end (GWB; Reddy et al., 2017) provides three different observation modes, namely IA, PA or CDPA, as described in Section 2. The settings used during a pulsar observation depend on the band of observation and the mode of the observatory back-end. These settings are required for data reduction using `pinta` and are communicated to the pipeline through a `pipeline.in` file as mentioned in Section 2.3. As the frequency labelling of the pulsar data cube varies with the back-end mode used, these need to be determined and encoded in `pinta` in a manner which simplifies the specification of observation settings for the user.

The times of arrival (TOAs) of a pulsar pulse recorded simultaneously in two bands A and B, using back-end modes P and Q respectively, are related by

$$t_{AP} - t_{BQ} = \Delta_{PQ} + \mathcal{D} \times \text{DM} (F_{1A}^{-2} - F_{1B}^{-2}), \quad (3)$$

where t_{AP} and t_{BQ} are the TOAs, Δ_{PQ} is the relative instrumental offset between modes P and Q, \mathcal{D} is the dispersion measure constant, DM is the dispersion measure of the pulsar at the epoch of observation, and F_{1A} and F_{1B} are the frequency labels of the channels to which the signals in bands A and B are dedispersed. Both the offsets Δ_{PQ} and the frequency labels F_1 are crucial for performing precision pulsar timing using uGMRT. These are defined as part of the engineering specifications of the GWB hardware and software (Reddy et al., 2017;

#JName	RawData	Timestamp	Freq	Nbin	NChan	BandWidth	TSmpl	SB	NPol	TSubint	Cohded
J1939+2134	J1939+2134.25032019.B3.cdp.dat	J1939+2134.25032019.B3.cdp.timestamp	500	128	1024	100	0.00008192	LSB	1	10.0	1
J1939+2134	J1939+2134.25032019.B4.pa.raw	J1939+2134.25032019.B4.pa.hdr	750	128	1024	100	0.00008192	LSB	1	10.0	0
J1939+2134	J1939+2134.25032019.B5.cdp.dat	J1939+2134.25032019.B5.cdp.timestamp	1460	128	1024	100	0.00008192	LSB	1	10.0	1

Figure 2. An example pipeline.in file

De & Gupta, 2016). Engineering tests with standard inputs to the hardware were carried out to verify these definitions, but astronomical tests with wideband radio emission are also needed to gain confidence, particularly for coherently dedispersed data. In this section, we describe astronomical tests carried out to validate the frequency labeling to be encoded in pinta, and to determine the offsets Δ_{PQ} .

3.1 Calibration experiment

The required frequency labeling and the instrumental offsets were validated using observations of the Crab pulsar (PSR J0534+2200) and PSR J0332+5434. The former is a bright pulsar with 33.7 ms period and a relatively high DM (56.7 pc cm^{-3} ; Lyne et al., 2014). The DM of the Crab pulsar varies from epoch to epoch and this pulsar exhibits sporadic intense pulses, called giant pulses (GPs; Lundgren et al., 1995; Hankins et al., 2003), typically once every 4 minutes. The GPs provide a time marker, which is a strong function of frequency due to dispersion in the inter-stellar medium. Moreover, the arrival times of this marker across different frequencies vary with epoch due to DM variations. Thus, GPs provide a sensitive probe to validate the assumed frequency labels for the spectral data. PSR J0332+5434 is the brightest pulsar in the northern hemisphere with a period of 714 ms and DM of 26.76 pc cm^{-3} . Bright single pulses with pulse-to-pulse intensity variations interspersed with pulse nulls are seen in this pulsar (see Figure 3a).

The GWB can simultaneously be used in its different modes of operation in different bands using any combination of the four beams provided (Gupta et al., 2017; Reddy et al., 2017). This capability was exploited to record data on Crab pulsar GPs and single pulses from PSR J0332+5434 in IA, PA, and CDPA modes of GWB using different frequency bands available with the uGMRT. We investigated the cross-correlation in the recorded time series from different modes to determine relative instrumental delays as well as frequency labeling of the pulsar data in different modes. The lag in the arrival times of GPs from Crab pulsar, recorded with PA in Band 5 and CDPA in Band 3, depends on the DM of the pulsar (specified up to a precision of 0.001 pc cm^{-3}) and the frequency labeling used for the two bands, as given by equation 3. The DM time series of this pulsar is known to the required precision from measurements

made public by the Jodrell Bank Observatory⁵ (Lyne et al., 1993, 2014). Hence, any difference between the expected and measured lags is due to either (a) wrong frequency labeling, or (b) relative time offset between the two modes. As the DM of this pulsar varies over a timescale of one month, two observations separated by one month will yield different delays due to frequency labeling, whereas the delay due to relative offset is expected to be constant. Thus, both the frequency labeling as well as relative offsets can be simultaneously determined by two such observations. We check these results for consistency using the two pulsars with different DMs.

3.2 Calibration observations and results

Observations were carried out on 2019 December 16 (MJD 58832), 2020 January 24 (MJD 58871), and 2020 May 22 (MJD 58991). The estimated lags for one combination of modes on 2020 January 24 are shown in Figures 3a and 3b. The relative offsets and frequency labeling were then determined by matching the measured and expected lags, given by equation (3), and the estimated relative offsets for different modes are tabulated in Table 3. The relative pipeline delays measured as a result of tests conducted in the first two epochs were corrected in the software by the GMRT engineering team in April 2020. This was verified in the tests conducted on May 22, 2020 as can be seen from Table 3.

The frequency labeling for the different modes are expressed in terms of the value of the highest frequency channel (F_1) in the following expressions:

For IA and PA,

$$F_1 = \begin{cases} F_{\text{LO}} & \text{for LSB} \\ F_{\text{LO}} + \Delta F & \text{for USB} \end{cases}, \quad (4a)$$

and for CDPA,

$$F_1 = \begin{cases} F_{\text{LO}} - \frac{\Delta F}{N_{\text{chan}}} & \text{for LSB} \\ F_{\text{LO}} + \Delta F \left(1 - \frac{1}{N_{\text{chan}}}\right) & \text{for USB} \end{cases}. \quad (4b)$$

Here, F_{LO} refers to the Local Oscillator (LO) frequency (MHz) used for the observations, ΔF is the acquisition bandwidth (typically 100 or 200 MHz) and N_{chan} denotes the number of channels or sub-bands across the band. The expression is different for each side-band denoted by USB or LSB. When F_{LO} is chosen at the lowest

⁵This time series may be found at <http://www.jb.man.ac.uk/pulsar/crab/crab2.txt> and is updated regularly.

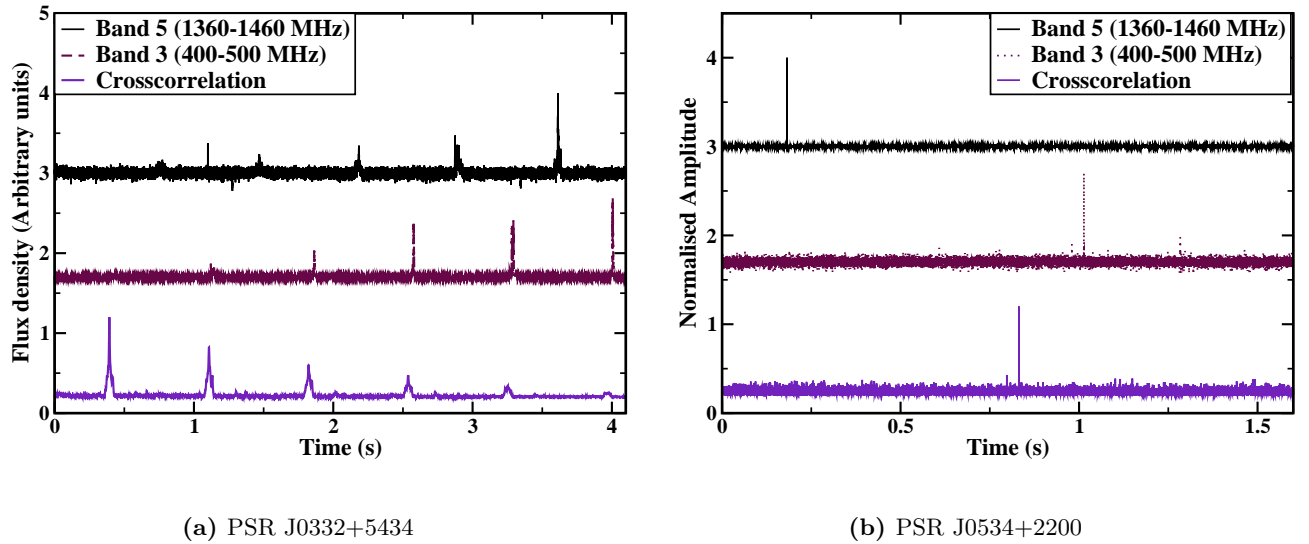


Figure 3. Time series observed using Band 5 (1360 – 1460 MHz : top plot in each panel) and Band 3 (400 – 500 MHz : middle plot in each panel) was used to determine the delay between the two bands using pulsars PSRs J0332+5434 and J0534+2200. The delay is obtained from the lag measured using the cross-correlation (shown in the bottom plot of each panel) of the two time series. The delay in each case was compared with that expected due to dispersion in ionised inter-stellar medium to determine both the frequency definition as well as relative pipeline delays : (a) Observations of single pulses of the bright pulsar J0332+5434 showing a delayed single pulse pattern in Band 3 compared to Band 4, (b) Observations of a Giant pulse of PSR J0534+2200 where the delay between Band 5 (top plot) and Band 3 (middle plot) was found consistent with that expected due to dispersion, assuming the correct frequency definitions (Equations 4a & 4b) and zero relative fixed pipeline delay.

edge of the band being used, this is called upper side-band (USB) where frequencies are ordered from lowest to highest frequency. The reverse order of frequencies are used in lower side-band (LSB) with the F_{LO} chosen at the highest edge of the band. Equations 4a-4b are in agreement with what is expected from the implementation of the IA, PA, and CDPA pipelines in GWB (Reddy et al., 2017; De & Gupta, 2016).

These equations are implemented in `pinta` to make it simpler for the user to use our data reduction pipeline. The user specifies the LO frequency, the side-band, the acquisition bandwidth and the number of sub-bands/channels in the `pipeline.in` file using the same values as specified for the back-end observation setup. The relative offsets determined in these experiments are not coded in `pinta`, but are included as part of TEMPO2 clock files used in the clock-chain for any timing analysis of the uGMRT data.

4 PERFORMANCE

To validate the pipeline and investigate its performance, we performed a series of tests using a variety of uGMRT datasets with varying data volume and observation frequencies. Specifically, we have sliced the raw data files from ten different observations (the details of these

datasets are given in Table 4) into file sizes of 1 GiB⁶, 2 GiB, 4 GiB, 8 GiB, 16 GiB and 32 GiB, processed each slice separately in `pinta`, and in each case recorded the execution time of each component of `pinta` as well as the total execution time. The result of this exercise is shown in Figure 4 where the ratio of the execution time to the observation duration (observe-to-reduce ratio) is plotted against the observation duration. Each point in Figure 4 represents the median of ten test cases and the error bar represents the corresponding median absolute deviation, and shows the observe-to-reduce ratio to be approximately between 1.5 and 3 and is not strongly dependent on the data volume. This behavior is desirable and the observe-to-reduce ratio can indeed be improved to be better than real-time by optimizing and parallelizing the pipeline, which we plan to do in the future. Such improvements can in principle allow `pinta` to be deployed as a real-time observatory pipeline for pulsar data reduction. We also note that the observe-to-reduce ratio while using only one of the two branches is close to or better than real-time.

4.1 RFI Mitigation

RFI mitigation is one of the most important processing steps in the `pinta` pipeline. In order to illustrate the

⁶1 GiB = 2³⁰ B.

Epoch (MJD)	DM (pc cm^{-3})	Bands and Modes	Sampling Time (μs)	Expected delay (s)	Observed delay (s)	Δ_{PQ} s
58832	56.7528	B5CDPA-B3CDPA	81.92	0.83172	0.83165(8)	0.0
		B3CDPA-B5PA	81.92	0.83173	0.83173(8)	1.34218
		B5CDPA-B5PA	81.92	0.00001	0.00008(8)	1.34226
		B5PA-B3PA	81.92	0.83137	0.83141(8)	0.0
58871	56.7401	B5CDPA-B3CDPA	20.48	0.83259	0.83259(2)	0.0
		B3CDPA-B5PA	81.92	2.1748	2.1746(2)	1.342177
		B5PA-B3PA	81.92	0.8312	0.8312(1)	0.0
58991	56.7781	B5CDPA-B3CDPA	5.12	0.8374	0.8375(1)	0.0
		B5CDPA-B4PA	40.96	0.39062	0.39051(8)	0.0
		B3CDPA-B4PA	40.96	0.4468	0.4470(2)	0.0
		B4PA-B5PA	40.96	0.4470	0.4472(2)	0.0
		B5PA-B5IA	40.96	0.0	0.0	0.0

Table 3 Results of time delay measurements simultaneously at two different frequency using PSR J0534+2200 for validating frequency definitions and relative pipeline delays (Δ_{PQ}) for different modes of pulsar observations. The epoch of observations is given in the first column along-with Dispersion measure at that epoch in second column followed by sampling time used, expected and observed delay in samples for different combination of modes at the two frequencies in fourth, fifth, sixth, seventh and third column respectively. The last column presents the relative pipeline delays (Δ_{PQ}). The abbreviations B5CDPA, B3CDPA, B5PA and B3PA indicate data acquisition using Band 5 in CDPA mode, using Band 3 in CDPA mode, Band 5 in PA mode, and Band 3 in PA mode respectively.

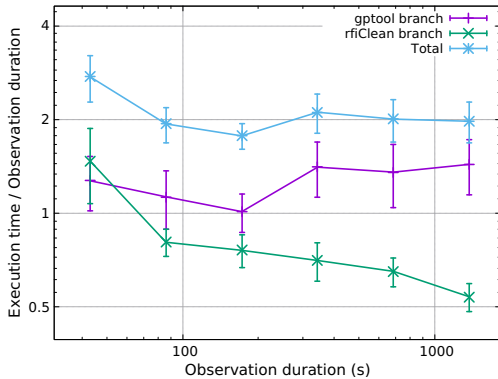


Figure 4. Ratio of execution time by observation duration (observe-to-reduce ratio) plotted versus the observation duration. The observe-to-reduce ratio for each of the two branches of `pinta` as well as the same for the entire pipeline is plotted. Each data point represents the median of 10 tests and the error bars represent the corresponding median absolute deviation.

RFI mitigation in the pipeline, we present here a study on ten different datasets (see Table 4), each having varying levels of RFI. Data segments were selected from the uGMRT observation bands 3-5, MJD 58260-58389 with a total length for the segments 11544 seconds. The data quality of each segment prior to and after the `pinta` RFI mitigation was studied. `rfifind` command of `PRESTO` (Ransom, 2011) was used to report the percentage of good intervals in the data. The percentage of good intervals that is gained after the RFI mitigation is shown (in red) in Figure 5. This study provides a feel for the typical RFI mitigation available in the pipeline.

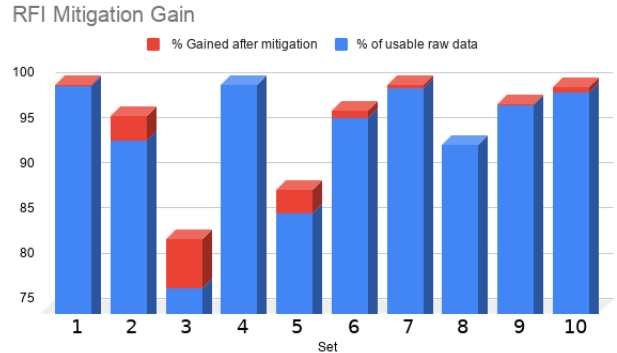


Figure 5. Effectiveness of RFI Mitigation. Each bar represents one dataset. The details of each dataset is given in Table 4.

5 SUMMARY AND DISCUSSION

We developed a pipeline to reduce uGMRT pulsar timing raw data for the InPTA experiment, named `pinta`, which reduces the raw data input to RFI-mitigated folded profile archives. Since the uGMRT raw data input does not contain any metadata such as the observation settings, they are provided to the pipeline via an ASCII input file named `pipeline.in`, whose contents are summarized in Table 2. `pinta` performs RFI mitigation using two different packages, namely `gptool` and `rfiClean`, running them in two different branches which produce two different output archives. `pinta` provides various command line options to control how these two branches are run, summarized in Table 1.

It is crucial to use the correct interpretation of the ob-

Dataset	Pulsar	Date	Band	Coherent Dedispersion
1	J1857+0943	25/08/2018	5	Yes
2	J2145-0750	22/05/2018	4	No
3	J2145-0750	25/08/2018	3	Yes
4	J2145-0750	10/09/2018	3	Yes
5	J1939+2134	21/05/2018	3	Yes
6	J1939+2134	28/09/2018	4	No
7	J1713+0747	07/06/2018	5	Yes
8	J2124-3358	10/09/2018	3	Yes
9	J1643-1224	08/07/2018	3	Yes
10	J1643-1224	25/08/2018	5	Yes

Table 4 The details of the datasets used for characterizing the performance and RFI mitigation efficacy of `pinta`. Bands 3, 4 and 5 represent 400–500 MHz, 650–750 MHz, and 1360-1460 MHz respectively for our observations.

servatory frequency settings while performing the data reduction. We performed validation and calibration experiments using GPs from the Crab pulsar and single pulses from the bright pulsar J0332+5434 to ensure that our interpretation of the observation frequency for IA, PA and CDPA pipelines of uGMRT matches what is given in equations (4a) and (4b). This experiment also allowed us to measure the instrumental delays between IA, PA and CDPA pipelines of uGMRT.

To characterize the computational performance of `pinta`, we conducted a number of tests using different datasets. These tests showed that the net observe-to-time ratio of `pinta` is approximately 2, while the observe-to-time ratio of individual branches is less than 1.5. These results lead us to strive to achieve real-time observe-to-time ratio by employing parallelization techniques to the pipeline. We also conducted tests to investigate the RFI mitigation efficacy of `pinta` on the same datasets, the results of which are shown in Figure 5. We observe that the RFI mitigation gains seen in different datasets, having different RFI characteristics, vary significantly as expected, with some datasets yielding up to $\sim 10\%$ gain RFI mitigation gain. These results substantiate the addition of RFI mitigation tools in `pinta`.

In the next section we briefly describe our future goals for the development of `pinta` as well as other related pipelines and codes relevant to the InPTA experiment.

6 FUTURE SCOPE

Our plans for the future development of `pinta` include the improvement of its computational efficiency to achieve better than real-time performance. This may be achieved by (a) running the two branches of the pipeline parallelly instead of serially, (b) modifying the `filterbank` program to use a GPU and (c) utilizing the GPU processing option in `dspsr`.

Similar pipelines for reducing the data obtained using the legacy GMRT and the ORT are also under

development, ensuring a high level of compatibility with `pinta`. In addition, we plan on developing “InPTA Data Management System”, a database for tracking metadata associated with the observations and data analysis of the InPTA experiment, which will be tightly integrated with `pinta` as well as the legacy GMRT and ORT pipelines.

7 ACKNOWLEDGEMENTS

We thank the staff of the GMRT who made our observations possible. GMRT is run by the National Centre for Radio Astrophysics of the Tata Institute of Fundamental Research. BCJ, YG and AB acknowledge the support of the Department of Atomic Energy, Government of India, under project # 12-R&D-TFR-5.02-0700. AS, AG and LD acknowledge the support of the Department of Atomic Energy, Government of India, under project # 12-R&D-TFR-5.02-0200. MPS acknowledges funding from the European Research Council (ERC) under the European Union’s Horizon 2020 research and innovation programme (grant agreement No. 694745). AC acknowledges the funding received from Department of Science and Technology, Government of India, WOS-A scheme, file no. SR/WOS-A/PM-26/2018.

REFERENCES

- Abbott B. P., et al., 2019, *Phys. Rev. X*, 9, 031040
Alam M. F., et al., 2020a, arXiv e-prints, [p. arXiv:2005.06490](https://arxiv.org/abs/2005.06490)
Alam M. F., et al., 2020b, arXiv e-prints, [p. arXiv:2005.06495](https://arxiv.org/abs/2005.06495)
Bailes M., et al., 2018, in Proceedings of MeerKAT Science: On the Pathway to the SKA — PoS(MeerKAT2016). p. 11, [doi:10.22323/1.277.0011](https://doi.org/10.22323/1.277.0011)
Berczik P., Merritt D., Spurzem R., Bischof H.-P., 2006, *The Astrophysical Journal*, 642, L21
Burke-Spolaor S., et al., 2019, *A&A Rev.*, 27, 5
Chowdhury A., Gupta Y., 2020, In preparation

- De K., Gupta Y., 2016, *Experimental Astronomy*, 41, 67
- Desvignes G., et al., 2016, *MNRAS*, 458, 3341
- Gupta Y., et al., 2017, *Current Science*, 113, 707
- Hamaker J. P., Bregman J. D., Sault R. J., 1996, *A&AS*, 117, 137
- Hankins T. H., Kern J. S., Weatherall J. C., Eilek J. A., 2003, *Nature*, 422, 141
- Hobbs G., 2013, *Classical and Quantum Gravity*, 30, 224007
- Hobbs G., Dai S., 2017, *National Science Review*, 4, 707
- Hobbs G., et al., 2010, *Classical and Quantum Gravity*, 27, 084013
- Hobbs G., et al., 2020, *MNRAS*, 491, 5951
- Hotan A. W., van Straten W., Manchester R. N., 2004, *Publications of the Astronomical Society of Australia*, 21, 302–309
- Joshi B. C., et al., 2018, *Journal of Astrophysics and Astronomy*, 39, 51
- Kerr M., et al., 2020, *Publications of the Astronomical Society of Australia*, 37, e020
- Kramer M., Champion D. J., 2013, *Classical and Quantum Gravity*, 30, 224009
- Lee K. J., 2016, in Qain L., Li D., eds, *Astronomical Society of the Pacific Conference Series Vol. 502, Frontiers in Radio Astronomy and FAST Early Sciences Symposium 2015*. Astronomical Society of the Pacific, p. 19, http://www.aspbooks.org/a/volumes/article_details/?paper_id=37688
- Lorimer D. R., 2011, *SIGPROC: Pulsar Signal Processing Programs* (ascl:1107.016)
- Lundgren S. C., Cordes J. M., Ulmer M., Matz S. M., Lomatch S., Foster R. S., Hankins T., 1995, *ApJ*, 453, 433
- Lyne A. G., Pritchard R. S., Graham Smith F., 1993, *Monthly Notices of the Royal Astronomical Society*, 265, 1003
- Lyne A. G., Jordan C. A., Graham-Smith F., Espinoza C. M., Stappers B. W., Weltevrede P., 2014, *Monthly Notices of the Royal Astronomical Society*, 446, 857
- Maan Y., Joshi B. C., Surnis M. P., Bagchi M., Manoharan P. K., 2019, *ApJL*, 882, L9
- Maan Y., Vohl D., van Leeuwen J., 2020, in prep.
- McLaughlin M. A., 2013, *Classical and Quantum Gravity*, 30, 224008
- Naidu A., Joshi B. C., Manoharan P. K., Krishnakumar M. A., 2015, *Experimental Astronomy*, 39, 319
- Oostrum L. C., van Leeuwen J., Maan Y., Coenen T., Ishwara-Chandra C. H., 2020, *MNRAS*, 492, 4825
- Pearson W. J., et al., 2019, *A&A*, 631, A51
- Perera B. B. P., et al., 2019, *Monthly Notices of the Royal Astronomical Society*, 490, 4666
- Ransom S., 2011, *ASCL.net Astrophysics Source Code Library*
- Reddy S. H., et al., 2017, *Journal of Astronomical Instrumentation*, 06, 1641011
- Susobhanan A., Gopakumar A., Hobbs G., Taylor S. R., 2020, *Phys. Rev. D*, 101, 043022
- Swarup G., et al., 1971, *Nature Physical Science*, 230, 185
- Swarup G., Ananthakrishnan S., Kapahi V. K., Rao A. P., Subrahmanya C. R., Kulkarni V. K., 1991, *Current Science*, 60, 95
- van Straten W., Bailes M., 2011, *PASA*, 28, 1
- van Straten W., Demorest P., Osłowski S., 2012, *Astronomical Research and Technology*, 9, 237